Acta Cryst E CRYSTALLOGRAPHIC COMMUNICATIONS

ISSN 2056-9890

Co-crystal sustained by π-type halogen-bonding interactions between 1,4-diiodoperchlorobenzene and naphthalene

Eric Bosch,[a] Eric W. Reinheimer,[b] Daniel K. Unruh[c] and Ryan H. Groeneman[d]*

[a]Department of Chemistry and Biochemistry, Missouri State University, Springfield, MO 65897, USA, [b]Rigaku Americas Corporation, The Woodlands, TX 77381, USA, [c]Office of the Vice President for Research, University of Iowa, Iowa City, IA 52242, USA, and [d]Department of Natural Sciences and Mathematics, Webster University, St. Louis, MO 63119, USA. *Correspondence e-mail: ryangroeneman19@webster.edu

Received 7 September 2023
Accepted 22 September 2023

Edited by J. Reibenspies, Texas A & M University, USA

Keywords: halogen bonding; co-crystal; Type I chlorine-chlorine contacts; Type II iodine-chlorine contacts.

CCDC reference: 2291675

Supporting information: this article has supporting information at journals.iucr.org/e

The formation and crystal structure of a co-crystal based upon 1,4-diiodoperchlorobenzene ($C_6I_2Cl_4$) as the halogen-bond donor along with naphthalene (nap) as the acceptor is reported. The co-crystal [systematic name: 1,2,4,5-tetrachloro-3,6-diiodobenzene–naphthalene, ($C_6I_2Cl_4$)·(nap)] generates a chevron-like structure that is held together primarily by π-type halogen bonds (*i.e.* C—I$\cdots\pi$ contacts) between the components. In addition, $C_6I_2Cl_4$ also interacts with the acceptor *via* C—Cl$\cdots\pi$ contacts that help stabilize the co-crystal. Within the solid, both aromatic components are found to engage in offset and homogeneous face-to-face π–π stacking interactions. Lastly, the halogen-bond donor $C_6I_2Cl_4$ is found to engage with neighboring donors by both Type I chlorine–chlorine and Type II iodine–chlorine contacts, which generates an extended structure.

1. Chemical context

Halogen bonding continues to be a highly utilized non-covalent interaction in the formation of multicomponent molecular solids such as co-crystals. Halogen bonding is an attractive interaction between an electrophilic region on a halogen atom and a nucleophilic region on a second atom (Gilday *et al.*, 2015). This electrophilic or positive region, namely the σ-hole, is located at the tip of a halogen atom bound to a carbon that interacts with a lone pair on an atom or an electron-rich aromatic surface (Cavallo *et al.*, 2016). In general, iodine generates the largest positive σ-hole when combined with neighboring electronegative atoms such as fluorine. The majority of these reported halogen bonds are classified as *n*-type meaning that the halogen atom is interacting with a lone pair such as on an N or O atom (Walsh *et al.*, 2001). A lesser investigated class of halogen bonds are π-type (*i.e.* C—I$\cdots\pi$ contacts) where the halogen atom interacts with an electron-rich surface such as a polycyclic aromatic hydrocarbon (Vainauskas *et al.*, 2020; d'Agostino *et al.*, 2015; Shen *et al.*, 2012).

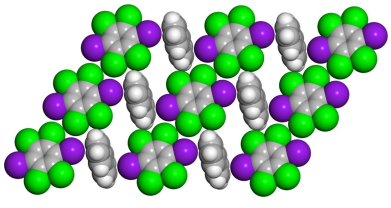

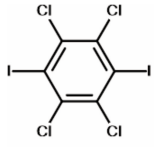

$C_6I_2Cl_4$

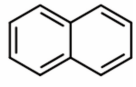

nap

A continued goal within our research groups has been in the design and formation of halogen-bonded co-crystals based

upon 1,4-diiodoperchlorobenzene ($C_6I_2Cl_4$) as the donor. Recently, we reported the formation of photoreactive co-crystals based upon $C_6I_2Cl_4$ along with *trans*-1,2-bis(pyridine-4-yl)ethylene (Bosch *et al.*, 2019*b*) and 4-stilbazole (Bosch *et al.*, 2019*c*) that are held together by primarily C—I···N or *n*-type halogen bonds. With the goal of expanding the type of halogen bonds that $C_6I_2Cl_4$ can form in molecular co-crystals, a study with a polycyclic aromatic was undertaken. Herein, we report the solid-state crystal structure of a co-crystal held together primarily by π-type halogen bonds between $C_6I_2Cl_4$ and naphthalene (nap) resulting in a chevron-like structure. In addition to the π-type halogen bond, the co-crystal $(C_6I_2Cl_4)\cdot(nap)$ is also held together by the combination of C—Cl···π contacts, homogeneous face-to-face π–π stacking interactions, Type I chlorine–chlorine contacts, and Type II iodine–chlorine contacts.

2. Structural commentary

Crystallographic analysis reveals that $(C_6I_2Cl_4)\cdot(nap)$ crystallizes in the centrosymmetric triclinic space group $P\overline{1}$. The asymmetric unit contains half a molecule of both $C_6I_2Cl_4$ and nap where inversion symmetry generates the remainder of each molecule (Fig. 1). The co-crystal is sustained by π-type or C—I···π halogen bonds with a distance of 3.373 (1) Å along with a nearly perpendicular halogen-bond angle of 90.99 (4)° (Fig. 2). This halogen-bond distance and angle were determined by using the I atom on $C_6I_2Cl_4$ and the calculated plane for the nap molecule. As expected, $C_6I_2Cl_4$ forms two π-type halogen bonds with two different nap molecules, generating a chevron-like pattern (Fig. 2).

3. Supramolecular features

In addition to π-type halogen bond within $(C_6I_2Cl_4)\cdot(nap)$, the donor $C_6I_2Cl_4$ is found to engage in Type I chlorine–chlorine contacts (Fig. 3). These interactions are found between crystallographically equivalent Cl atoms, namely Cl2···Cl2^{i} [symmetry code: (i) $1-x$, $-y$, $1-z$], with a distance of 3.499 (1) Å and a C—Cl···Cl bond angle of $\theta_1 = \theta_2 =$ 132.16 (6)° (Mukherjee *et al.*, 2014; Desiraju & Parthasarathy, 1989). In addition, neighboring donors also interact *via* Type II iodine–chlorine contacts. This interaction is found between I1···Cl2^{i} [symmetry code: (i) $1-x$, $-y$, $1-z$], with a distance of 3.808 (1) Å and a C—I···Cl bond angle of 111.83 (4)°. Both the aromatic halogen-bond donor and acceptor are found to engage in an offset and homogeneous face-to-face π–π stacking arrangement that stabilizes the co-crystal (Fig. 3). Lastly, $C_6I_2Cl_4$ is interacting with two additional nap molecules *via* C—Cl···π contacts at a distance of 3.391 (2) Å measured for Cl1···C5.

These various non-covalent interactions were also investigated and visualized by utilizing a Hirshfeld surface analysis (Spackman *et al.*, 2021) where d_{norm} is mapped onto the calculated surface (Fig. 4). The darkest red spots on the Hirshfeld surface represents the shortest van der Waals contacts where the π-type halogen bond is located. In addition, the faint red spots indicate separations less than the sum of the van der Waals radii for the C—Cl···π contacts. Lastly, dashed lines illustrate the Type I chlorine–chlorine interactions observed within $(C_6I_2Cl_4)\cdot(nap)$. This Hirshfeld

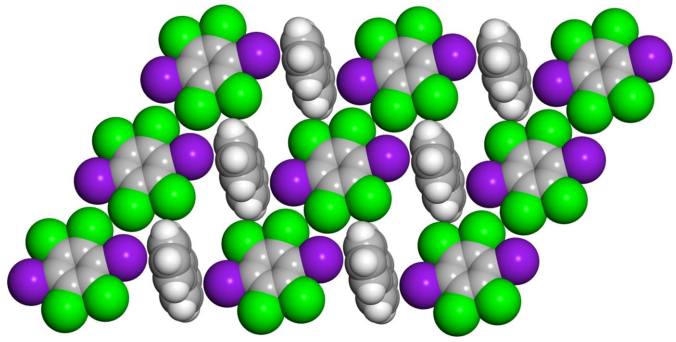

Figure 2
X-ray crystal structure of $(C_6I_2Cl_4)\cdot(nap)$ illustrating the chevron-like packing pattern along with π-type halogen bonds. In addition, the Type I chlorine–chlorine and Type II iodine–chlorine interactions between neighboring chevron-based chains are also shown.

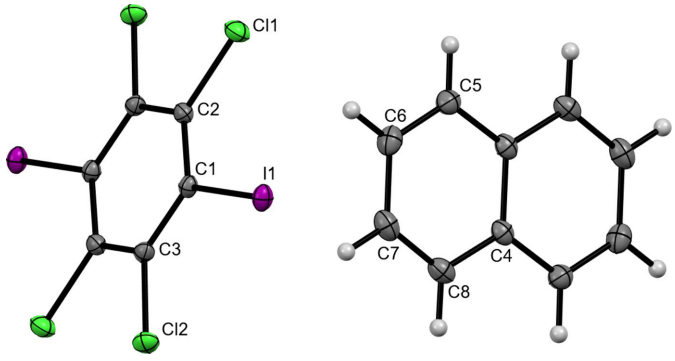

Figure 1
The labeled asymmetric unit of $(C_6I_2Cl_4)\cdot(nap)$. Displacement ellipsoids are drawn at the 50% probability level for non-hydrogen atoms while hydrogen atoms are shown as spheres of arbitrary size.

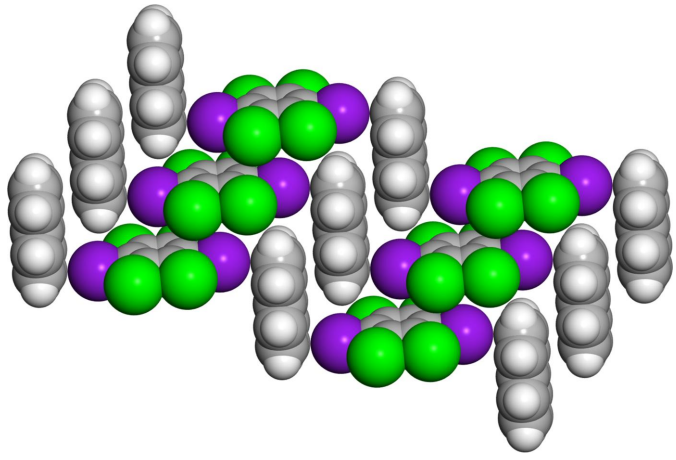

Figure 3
X-ray crystal structure of $(C_6I_2Cl_4)\cdot(nap)$ illustrating the π-type halogen bonds and the offset face-to-face stacking of both the halogen-bond donor and acceptor.

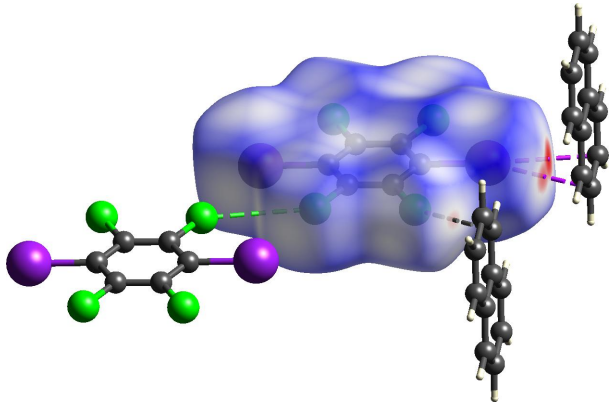

Figure 4
Hirshfeld surface of $(C_6I_2Cl_4)\cdot(nap)$ where d_{norm} is mapped onto the surface illustrating the π-type halogen bonds (darkest red spots) and C—Cl$\cdots\pi$ contacts (faint red spots). Lastly, the Type I chlorine–chlorine interactions are shown with green dashed lines.

surface analysis along with the observed bond lengths confirms the ability of $C_6I_2Cl_4$ to engage in π-type halogen bonds to a polycyclic aromatic hydrocarbon, namely nap.

4. Database survey

A search of the Cambridge Crystallographic Database (Version 2023.2.0 Build 3382240; Groom *et al.*, 2016) using *Conquest* (Bruno *et al.*, 2002) for structures containing 1,4-diiodoperchlorobenzene ($C_6I_2Cl_4$) in which the I atom is within the van der Waals radius of an aromatic surface revealed only one structure, refcode HONBIY (Bosch, 2019*a*). In particular, this multicomponent solid is a monosolvate of benzene where $C_6I_2Cl_4$ forms two π-type halogen bonds, generating a similar chevron-like pattern observed in $(C_6I_2Cl_4)\cdot(nap)$.

5. Synthesis and crystallization

Materials and general methods

The solvent toluene along with the halogen-bond acceptor naphthalene (nap) were both purchased from Sigma-Aldrich Chemical (St. Louis, MO, USA) and used without any additional purification. The halogen-bond donor 1,4-diiodoperchlorobenzene ($C_6I_2Cl_4$) was synthesized utilizing a previously published method (Reddy *et al.*, 2006).

Synthesis and crystallization

The formation of $(C_6I_2Cl_4)\cdot(nap)$ was achieved by dissolving 50.0 mg of $C_6I_2Cl_4$ in 2.0 mL of toluene and then combined with a 2.0 mL toluene solution containing 13.7 mg of nap (1:1 molar equivalent). Within two days, single crystals suitable for X-ray diffraction were formed upon loss of some of the solvent by slow evaporation.

6. Refinement

Crystal data, data collection, and structure refinement details are summarized in Table 1. Intensity data were corrected for Lorentz, polarization, and background effects using *APEX4* (Bruker, 2021). Hydrogen atoms bound to carbon atoms were located in the difference Fourier map and were geometrically constrained using the appropriate AFIX commands.

Table 1
Experimental details.

Crystal data	
Chemical formula	$C_6Cl_4I_2\cdot C_{10}H_8$
M_r	595.82
Crystal system, space group	Triclinic, $P\overline{1}$
Temperature (K)	100
a, b, c (Å)	5.4830 (7), 6.4533 (11), 12.171 (2)
α, β, γ (°)	87.274 (5), 85.912 (5), 82.629 (9)
V (Å^3)	425.68 (12)
Z	1
Radiation type	Mo $K\alpha$
μ (mm^{-1})	4.31
Crystal size (mm)	0.14 × 0.12 × 0.10
Data collection	
Diffractometer	Bruker D8 Venture Duo with Photon III
Absorption correction	Multi-scan (*SADABS*; Krause *et al.*, 2015)
T_{min}, T_{max}	0.626, 0.746
No. of measured, independent and observed [$I > 2\sigma(I)$] reflections	30681, 2518, 2465
R_{int}	0.050
(sin $\theta/\lambda)_{max}$ (Å^{-1})	0.717
Refinement	
$R[F^2 > 2\sigma(F^2)]$, $wR(F^2)$, S	0.017, 0.038, 1.09
No. of reflections	2518
No. of parameters	100
H-atom treatment	H-atom parameters constrained
$\Delta\rho_{max}$, $\Delta\rho_{min}$ (e Å^{-3})	0.77, −0.47

Computer programs: *APEX4* (Bruker, 2021), *SAINT* (Bruker, 2016), *SHELXT2018/2* (Sheldrick, 2015*a*), *SHELXL* (Sheldrick, 2015*b*), and *OLEX2* (Dolomanov *et al.*, 2009).

Funding information

RHG gratefully acknowledges financial support from Webster University in the form of various Faculty Research Grants.

References

Bosch, E. (2019*a*). *IUCrData*, **4**, x190993.
Bosch, E., Kruse, S. J., Krueger, H. R. & Groeneman, R. H. (2019*b*). *Cryst. Growth Des.* **19**, 3092–3096.
Bosch, E., Kruse, S. J., Reinheimer, E. W., Rath, N. P. & Groeneman, R. H. (2019*c*). *CrystEngComm*, **21**, 6671–6675.
Bruker (2016). *SAINT*. Bruker AXS Inc., Madison, Wisconsin, USA.
Bruker (2021). *APEX4*. Bruker AXS Inc., Madison, Wisconsin, USA.
Bruno, I. J., Cole, J. C., Edgington, P. R., Kessler, M., Macrae, C. F., McCabe, P., Pearson, J. & Taylor, R. (2002). *Acta Cryst.* B**58**, 389–397.
Cavallo, G., Metrangolo, P., Milani, R., Pilati, T., Priimagi, A., Resnati, G. & Terraneo, G. (2016). *Chem. Rev.* **116**, 2478–2601.
d'Agostino, S, Grepioni, F., Braga, D. & Ventura, B. (2015). *Cryst. Growth Des.* **15**, 2039–2045.
Desiraju, G. R. & Parthasarathy, R. (1989). *J. Am. Chem. Soc.* **111**, 8725–8726.
Dolomanov, O. V., Bourhis, L. J., Gildea, R. J., Howard, J. A. K. & Puschmann, H. (2009). *J. Appl. Cryst.* **42**, 339–341.
Gilday, L. C., Robinson, S. W., Barendt, T. A., Langton, M. J., Mullaney, B. R. & Beer, P. D. (2015). *Chem. Rev.* **115**, 7118–7195.

Groom, C. R., Bruno, I. J., Lightfoot, M. P. & Ward, S. C. (2016). *Acta Cryst.* B**72**, 171–179.
Krause, L., Herbst-Irmer, R., Sheldrick, G. M. & Stalke, D. (2015). *J. Appl. Cryst.* **48**, 3–10.
Mukherjee, A., Tothadi, S. & Desiraju, G. R. (2014). *Acc. Chem. Res.* **47**, 2514–2524.
Reddy, C. M., Kirchner, M. T., Gundakaram, R. C., Padmanabhan, K. A. & Desiraju, G. R. (2006). *Chem. Eur. J.* **12**, 2222–2234.
Sheldrick, G. M. (2015*a*). *Acta Cryst.* A**71**, 3–8.
Sheldrick, G. M. (2015*b*). *Acta Cryst.* C**71**, 3–8.
Shen, Q. J., Pang, X., Zhao, X. R., Gao, H. Y., Sun, H.-L. & Jin, W. J. (2012). *CrystEngComm*, **14**, 5027–5034.
Spackman, P. R., Turner, M. J., McKinnon, J. J., Wolff, S. K., Grimwood, D. J., Jayatilaka, D. & Spackman, M. A. (2021). *J. Appl. Cryst.* **54**, 1006–1011.
Vainauskas, J., Topić, F., Bushuyev, O. S., Barrett, C. J. & Friščić, T. (2020). *Chem. Commun.* **56**, 15145–15148.
Walsh, R. B., Padgett, C. W., Metrangolo, P., Resnati, G., Hanks, T. W. & Pennington, W. T. (2001). *Cryst. Growth Des.* **1**, 165–175.

supporting information

Acta Cryst. (2023). E**79**, 958-961 [https://doi.org/10.1107/S2056989023008356]

Co-crystal sustained by π-type halogen-bonding interactions between 1,4-diiodoperchlorobenzene and naphthalene

Eric Bosch, Eric W. Reinheimer, Daniel K. Unruh and Ryan H. Groeneman

Computing details

Data collection: *APEX4* (Bruker, 2021); cell refinement: *SAINT* V8.40B (Bruker, 2016); data reduction: *SAINT* V8.40B (Bruker, 2016); program(s) used to solve structure: *SHELXT2018/2* (Sheldrick, 2015a); program(s) used to refine structure: *SHELXL* (Sheldrick, 2015b); molecular graphics: Olex2 1.5 (Dolomanov *et al.*, 2009); software used to prepare material for publication: Olex2 1.5 (Dolomanov *et al.*, 2009).

1,2,4,5-Tetrachloro-3,6-diiodobenzene–naphthalene (1/1)

Crystal data

$C_6Cl_4I_2 \cdot C_{10}H_8$
M_r = 595.82
Triclinic, $P\overline{1}$
a = 5.4830 (7) Å
b = 6.4533 (11) Å
c = 12.171 (2) Å
α = 87.274 (5)°
β = 85.912 (5)°
γ = 82.629 (9)°
V = 425.68 (12) Å^3
Z = 1
$F(000)$ = 278
D_x = 2.324 Mg m^{-3}
Mo $K\alpha$ radiation, λ = 0.71073 Å
Cell parameters from 9944 reflections
θ = 3.2–30.6°
μ = 4.31 mm^{-1}
T = 100 K
Irregular, clear colourless
0.14 × 0.12 × 0.10 mm

Data collection

Bruker D8 Venture Duo with Photon III diffractometer
phi and ω scans
Absorption correction: multi-scan (SADABS; Krause *et al.*, 2015)
T_{min} = 0.626, T_{max} = 0.746
30681 measured reflections
2518 independent reflections
2465 reflections with $I > 2\sigma(I)$
R_{int} = 0.050
θ_{max} = 30.7°, θ_{min} = 3.2°
h = −7→7
k = −9→9
l = −17→17

Refinement

Refinement on F^2
Least-squares matrix: full
$R[F^2 > 2\sigma(F^2)]$ = 0.017
$wR(F^2)$ = 0.038
S = 1.09
2518 reflections
100 parameters
0 restraints
Primary atom site location: dual
Hydrogen site location: inferred from neighbouring sites
H-atom parameters constrained
$w = 1/[\sigma^2(F_o^2) + 0.4448P]$ where $P = (F_o^2 + 2F_c^2)/3$
$(\Delta/\sigma)_{max}$ = 0.001
$\Delta\rho_{max}$ = 0.77 e Å^{-3}
$\Delta\rho_{min}$ = −0.47 e Å^{-3}

Special details

Geometry. All esds (except the esd in the dihedral angle between two l.s. planes) are estimated using the full covariance matrix. The cell esds are taken into account individually in the estimation of esds in distances, angles and torsion angles; correlations between esds in cell parameters are only used when they are defined by crystal symmetry. An approximate (isotropic) treatment of cell esds is used for estimating esds involving l.s. planes.

Refinement. A numerical absorption correction was applied based on a Gaussian integration over a multifaceted crystal and followed by a semi-empirical correction for adsorption applied using SADABS (Bruker, 2016). The program SHELXT (Sheldrick, 2015a) was used for the initial structure solution and SHELXL (Sheldrick, 2015b) was used for the refinement of the structure. Both programs were utilized within the OLEX2 software (Dolomanov *et al.*, 2009).

Fractional atomic coordinates and isotropic or equivalent isotropic displacement parameters (Å²)

	x	*y*	*z*	U_{iso}*/U_{eq}
I1	0.56547 (2)	0.30084 (2)	0.68774 (2)	0.01552 (4)
Cl1	0.87192 (8)	0.70258 (6)	0.72721 (3)	0.01816 (8)
Cl2	0.73398 (7)	0.12959 (6)	0.43367 (3)	0.01748 (8)
C1	0.8224 (3)	0.4211 (2)	0.57480 (12)	0.0125 (3)
C2	0.9407 (3)	0.5897 (2)	0.60178 (12)	0.0130 (3)
C3	0.8824 (3)	0.3322 (2)	0.47217 (12)	0.0127 (3)
C4	0.5015 (3)	0.0935 (3)	1.02907 (13)	0.0161 (3)
C5	0.3321 (3)	0.2714 (3)	1.00359 (14)	0.0187 (3)
H5	0.333552	0.396640	1.041387	0.022*
C6	0.1657 (3)	0.2649 (3)	0.92489 (15)	0.0214 (3)
H6	0.053127	0.385222	0.908670	0.026*
C7	0.1621 (3)	0.0800 (3)	0.86822 (14)	0.0209 (3)
H7	0.046094	0.076467	0.814172	0.025*
C8	0.3245 (3)	−0.0955 (3)	0.89020 (14)	0.0189 (3)
H8	0.320044	−0.218777	0.851101	0.023*

Atomic displacement parameters (Å²)

	U^{11}	U^{22}	U^{33}	U^{12}	U^{13}	U^{23}
I1	0.01377 (6)	0.01772 (6)	0.01506 (6)	−0.00420 (4)	0.00031 (3)	0.00367 (3)
Cl1	0.02229 (18)	0.01951 (17)	0.01340 (16)	−0.00507 (14)	0.00101 (13)	−0.00473 (13)
Cl2	0.01990 (17)	0.01571 (16)	0.01881 (17)	−0.00845 (13)	−0.00281 (13)	−0.00202 (13)
C1	0.0122 (6)	0.0126 (6)	0.0128 (6)	−0.0027 (5)	−0.0011 (5)	0.0018 (5)
C2	0.0143 (6)	0.0132 (6)	0.0115 (6)	−0.0013 (5)	−0.0023 (5)	−0.0010 (5)
C3	0.0129 (6)	0.0119 (6)	0.0139 (6)	−0.0032 (5)	−0.0032 (5)	0.0007 (5)
C4	0.0150 (7)	0.0205 (7)	0.0129 (6)	−0.0037 (6)	0.0019 (5)	−0.0007 (6)
C5	0.0200 (7)	0.0180 (7)	0.0177 (7)	−0.0022 (6)	0.0023 (6)	−0.0008 (6)
C6	0.0191 (8)	0.0224 (8)	0.0208 (8)	0.0013 (6)	0.0015 (6)	0.0030 (6)
C7	0.0171 (7)	0.0299 (9)	0.0162 (7)	−0.0048 (6)	−0.0015 (6)	−0.0004 (6)
C8	0.0177 (7)	0.0246 (8)	0.0156 (7)	−0.0066 (6)	0.0004 (6)	−0.0035 (6)

Geometric parameters (Å, º)

I1—C1	2.0929 (15)	C4—C8^{ii}	1.419 (2)
Cl1—C2	1.7196 (16)	C5—H5	0.9500
Cl2—C3	1.7252 (16)	C5—C6	1.374 (3)

C1—C2	1.399 (2)	C6—H6	0.9500
C1—C3	1.400 (2)	C6—C7	1.410 (3)
C2—C3^{i}	1.401 (2)	C7—H7	0.9500
C4—C4^{ii}	1.430 (3)	C7—C8	1.376 (3)
C4—C5	1.418 (2)	C8—H8	0.9500
C2—C1—I1	120.33 (11)	C4—C5—H5	119.6
C2—C1—C3	118.93 (13)	C6—C5—C4	120.84 (16)
C3—C1—I1	120.74 (11)	C6—C5—H5	119.6
C1—C2—Cl1	120.19 (12)	C5—C6—H6	120.0
C1—C2—C3^{i}	120.74 (14)	C5—C6—C7	120.05 (16)
C3^{i}—C2—Cl1	119.07 (11)	C7—C6—H6	120.0
C1—C3—Cl2	120.49 (12)	C6—C7—H7	119.6
C1—C3—C2^{i}	120.33 (13)	C8—C7—C6	120.82 (16)
C2^{i}—C3—Cl2	119.16 (11)	C8—C7—H7	119.6
C5—C4—C4^{ii}	119.00 (19)	C4^{ii}—C8—H8	119.8
C5—C4—C8^{ii}	122.12 (15)	C7—C8—C4^{ii}	120.41 (16)
C8^{ii}—C4—C4^{ii}	118.88 (19)	C7—C8—H8	119.8
I1—C1—C2—Cl1	−1.15 (18)	C3—C1—C2—C3^{i}	−0.4 (2)
I1—C1—C2—C3^{i}	178.35 (11)	C4^{ii}—C4—C5—C6	0.5 (3)
I1—C1—C3—Cl2	3.33 (18)	C4—C5—C6—C7	−0.1 (3)
I1—C1—C3—C2^{i}	−178.35 (11)	C5—C6—C7—C8	−0.3 (3)
C2—C1—C3—Cl2	−177.92 (11)	C6—C7—C8—C4^{ii}	0.2 (3)
C2—C1—C3—C2^{i}	0.4 (2)	C8^{ii}—C4—C5—C6	179.92 (16)
C3—C1—C2—Cl1	−179.91 (11)		

Symmetry codes: (i) −*x*+2, −*y*+1, −*z*+1; (ii) −*x*+1, −*y*, −*z*+2.